Marie Simonnet, Nicole Barré, Romuald Drot, Claire Le Naour, Vladimir Sladkov and Sylvie Delpech*

Multiparametric study of thorium oxide dissolution in aqueous media

DOI 10.1515/ract-2016-2607
Received March 22, 2016; accepted May 23, 2016; published online July 2, 2016

Abstract: Thorium oxide is poorly soluble: unlike uranium oxide, concentrated nitric acid medium is not sufficient to get quantitative dissolution. Addition of small amounts of fluoride is required to achieve thorium oxide total dissolution. The effect of several parameters on thorium oxide dissolution in order to optimize the dissolution conditions is reported in this paper. Thus the influence of solid characteristics, dissolution method, temperature and composition of dissolution medium on ThO_2 dissolution rate has been studied. No complexing agents tested other than fluoride allows total dissolution. Beyond a given HF concentration a decrease of the dissolution rate is observed due to the formation of a precipitate at the solid/solution interface. It was demonstrated by XPS measurements that this precipitate is constituted of thorium fluoride (ThF_4) formed during the ThO_2 dissolution. The low concentration of HF required to achieve a total dissolution and the activation energy value measured tends to show a catalytic effect of HF on the dissolution process.

Keywords: Thorium oxide, dissolution, dissolution parameters, thorium fluoride.

1 Introduction

Due to the increasing energy demand and diminishing fuel resources, alternative energy sources are being intensively researched. In the nuclear industry, more countries are showing an increased interest in exploiting thorium as a nuclear fuel. Indeed, at the beginning of the nuclear research, thorium oxide was considered as a potential solid nuclear fuel for power plants. In the early 1960s, several experiments with thorium fuels were carried out, yielding most of the currently used data on in-core fuel behavior and reprocessing process [1–3]. However, the thorium fuel cycle project was abandoned because of several issues. Firstly, addition of fissile elements to the fuel is required to initiate the nuclear reaction because natural thorium is only composed of a fertile isotope, ^{232}Th. Secondly, due to the production of ^{232}U, which decays in several heavy γ-emitter elements, the fuel requires specific shielding for the transport and the reprocessing steps. Lastly, recycling thorium oxide fuel is more difficult than reprocessing uranium one. Unlike uranium oxide, thorium oxide does not dissolve in concentrated nitric acid, so diluted solutions of fluoride compounds are added to the dissolution medium of the reprocessing process called THOREX [4]. The resulting mixture is highly corrosive, and 6–10 h are required for total dissolution. In order to improve dissolution stage, recent studies have tried to change the dissolution medium (trimethanesulfonic acid [5] and phosphoric acid [6]) or technique (autoclave and microwaves [6, 7], pyrochemistry [8]) but the proposed processes are either not really suitable for industrial purposes due to safety reasons, or require more technological advances for the scaling-up.

The aim of this paper is to study the influence of several important dissolution parameters to determine their effects on dissolution rate. Three main parameters have been studied: solid characteristics, dissolution media and dissolution methods.

2 Chemical reagents, materials and equipment

Thorium oxide has been synthesized from thorium nitrate powder ($Th(NO_3)_4$,$4H_2O$ by PROLABO) and oxalic acid solutions prepared from Fluka di-hydrated oxalate powder and deionized water. Concentrations of acids in dissolution media have been varied from 1 M to 10 M for nitric acid and from 0.5 mM to 50 mM for hydrofluoric acid. Solutions have been prepared by dilution of 69% nitric

***Corresponding author: Sylvie Delpech,** Institut de Physique Nucléaire, CNRS-IN2P3, Univ. Paris-Sud, Université Paris-Saclay, 91406 Orsay Cedex, France, E-mail: delpech@ipno.in2p3.fr
Marie Simonnet, Nicole Barré, Romuald Drot, Claire Le Naour and Vladimir Sladkov: Institut de Physique Nucléaire, CNRS-IN2P3, Univ. Paris-Sud, Université Paris-Saclay, 91406 Orsay Cedex, France

Brought to you by | Karlsruher Institut für Technologie KIT-Bibliothek
Authenticated
Download Date | 6/6/18 7:47 PM

acid and 40% hydrofluoric acid Sigma Aldrich suprapur reagents.

X-ray diffraction (XRD) patterns have been collected by an X-ray powder Diffractometer (D8 Advance Bruker AXS) in a Bragg–Brentano geometry (θ–θ) equipped with Cu radiation ($K_{\alpha 1,2}$ = 1.54178 Å). Phase identification was performed with the DIFFRACPlus 2013 software (version 16, Bruker AXS) and powder diffraction files (ICDD PDF4+ 2013).

Specific surface area measurements have been performed on a Coulter SA3100 (Beckman) using the BET method with nitrogen gas. XPS spectra have been obtained by a Thermo Scientific K_α apparatus with a focused monochromatic source (Al K_α = 1486.7 eV) and a hemispherical analyser (constant analyser energy mode). An ICP-OES Agilent 700 and a Shimadzu UV/Vis spectrometer have been used for solution analyses. Both methods require calibrations which have been made by dilution of standard thorium nitrate solutions provided by Inorganic Ventures.

3 Results

3.1 ThO_2 synthesis

A multi-parametric study requires the use of a large amount of homogeneous substrate. Thus, thorium oxide powder was synthesized in the lab by batches of 8 g and every set of experiments was done on oxide from the same batch. Considering the quantity of radioactive materials, the synthesis has to be performed in a glove box. Moreover, as the aim of the present paper was not to get the influence of sintering on ThO_2 dissolution, only powder has been studied here.

3.1.1 Synthesis: experimental protocol

The experimental protocol is summarized in Table 1. The wet route synthesis with oxalate precursors was chosen because it yields better crystallized oxides, and this experimental protocol can be achieved in a glove box. We applied one of the protocols used by Heisbourg et al. [9] and Hingant et al. [10], in which thorium oxalate was obtained by dripping oxalic acid on a concentrated thorium nitrate solution with a peristaltic pump while stirring at room temperature. Once washed with distilled water to eliminate the excess of acid, the powder is dried at 60°C for few days and then heated at 400°C for 5 h to remove sorbed water (by the two dehydration steps given Table 1), to decompose oxalates in CO, CO_2 and to get amorphous ThO_2. To obtain better crystallization, a second thermal treatment (calcination) at higher temperature is applied for 10 h. The range of chosen temperatures is from 850°C to 1500°C.

Table 1: Experimental protocol of thorium oxide powder synthesis.

Step 1	Thorium oxalate precipitation by dripping oxalic acid on thorium nitrate
	$Th^{4+} + 2\ H_2C_2O_4 + (4+n)\ H_2O \rightarrow Th(C_2O_4)_2, nH_2O + 4\ H_3O^+$
	$(2 < n < 6)$
Step 2	Oven drying (T = 60°C)
	$Th(C_2O_4)_2, nH_2O \rightarrow Th(C_2O_4)_2, 2H_2O$
Step 3	Heat treatment (T = 400°C)
	First dehydration step
	$Th(C_2O_4)_2, 2H_2O \rightarrow Th(C_2O_4)_2, H_2O + H_2O$
	Second dehydration step
	$Th(C_2O_4)_2, H_2O \rightarrow Th(C_2O_4)_2 + H_2O$
	Oxalate decomposition to obtain amorphous thorium oxide
	$Th(C_2O_4)_2 \rightarrow ThO_{2(s)} + 2CO(g) + 2CO_{2(g)}$
Step 4	Thorium oxide crystallization through thermal treatment
	$(850 < T < 1500°C)$
	ThO_2 (am) → ThO_2 (cr)

3.1.2 Synthesis: solid characterization

The calcination temperature is a key parameter that influences crystal characteristics such as grain size, specific surface area [10–12] or density [13], which are parameters impacting on ThO_2 dissolution kinetics [9]. To modify the oxides morphology, the thermal treatment was made at different temperatures, ranging from 850°C to 1500°C. To quantify the possible changes, two techniques, XRD and specific surface area measurements by BET [14] were chosen.

3.1.2.1 XRD acquisition

XRD patterns have been systematically recorded on freshly synthesized oxides to check their purity. The full width at half maximum (FWHM), which usually characterizes the crystallinity of a solid, is inversely proportional to the crystallite size and depends on heating temperature. When the calcination temperature increases from 1000°C to 1500°C, the FWHM clearly diminishes, showing that the crystallinity is improved. Progression in peak slimming is shown on Figure 1. From 1200°C, the resolution becomes good enough to observe the discrimination between the $K_{\alpha 1}$ and $K_{\alpha 2}$ peaks. The size of the crystallite was evaluated using the software DIFFRAC^{plus} (Bruker) based on the Sherrer formula and the results obtained are given Table 2. As expected, an increase of the size of crystallites with the temperature is observed.

Brought to you by | Karlsruher Institut für Technologie KIT-Bibliothek
Authenticated
Download Date | 6/6/18 7:47 PM

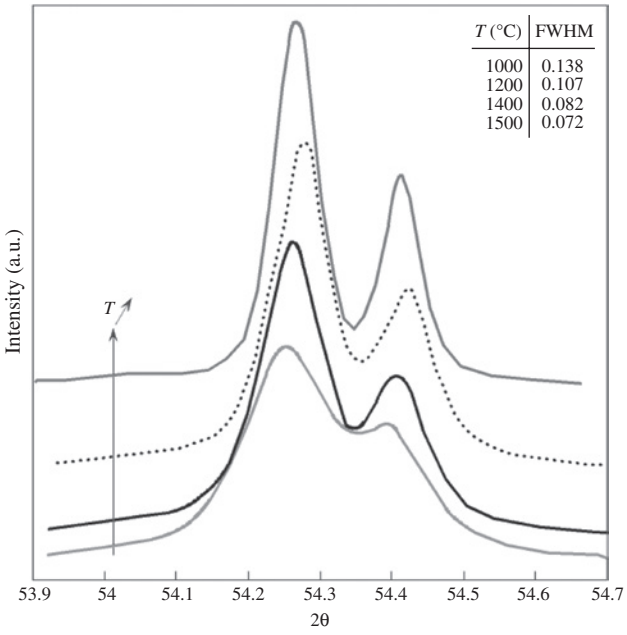

Figure 1: Evolution of line width ([311] diffraction plane) with the heating temperature. The FWHM values reported in the table correspond to $K_{\alpha 1}$ radiation.

Being that the aim of this study is the determination of optimal parameters towards thorium oxide dissolution, we have chosen to work with the substrate which presents a good crystallinity. Thus, in the following, all the dissolution studies have been performed considering solids heated at 1200°C except for the study on specific surface area influence towards dissolution.

3.1.2.2 BET measurements

The specific surface area is a fundamental parameter in dissolution experiments as the studied processes occur at the solid–solution interface [6, 15–17]. Moreover, this parameter is generally reported in the literature [6, 15–17] which allows one to compare the solids synthesized in this study with those used in previous studies. BET method with N_2 adsorption was used to measure the specific surface area of the synthesized powders. Previous work has demonstrated that the use of N_2 gas leads to equivalent results as water for specific surface area measurements of oxide or oxide-like compounds [18]. Results of BET measurements are given in Table 3, showing that specific surface area decreases with heating temperature increasing, which is consistent with the literature data [9]. Indeed, while the calcination temperature increases, the crystal grains growth, leading to a decrease in porosity. This result is perfectly correlated with XRD studies.

3.2 ThO_2 dissolution

3.2.1 Experimental protocols and methodology

Weighed amounts of ThO_2 powder are placed in Teflon beakers with aqueous media of the desired composition. For most studies, mass-over-volume ratio has been fixed at 6.5 g/L. It is obtained by adding 130 mg of ThO_2 to 20 mL of the dissolution media. Dissolution experiments are realized either under magnetic stirring and heating. Temperature is monitored by circulating thermostated oil. In the literature both mass/volume and surface/volume ratios are used to compare the dissolution tests. We have chosen to consider the mass/volume ratio in this paper because this term can be measured throughout the test.

Dissolution is quantified by measuring the thorium concentration in the aqueous phase as a function of dissolution time. Aliquots of 500 µL are removed every 2.5 min and centrifuged for 10 min. The number of withdrawals is between three and six depending on the dissolution experimental conditions. The total volume difference, which does not exceed 2 mL, is taken into account in the calculations after analyses. After centrifugation, 50 µL of the supernatant is diluted with 4.95 mL of 1 M HNO_3. Thorium concentration in the obtained solutions is then measured either by ICP-OES, with a calibration ranging from 0.5 mg/L to 100 mg/L or by UV/Vis spectrophotometry after complexation with the dye Arsenazo III reagent. This latter method has been achieved by using the Haleem Khan et al. [19] experimental protocol. From these results, the dissolved mass percentage ($\%ThO_2diss$) is calculated using the following formula:

$$\%ThO_2diss = 100 * \frac{C * V}{m} \quad (1)$$

Table 2: Evolution of the crystallite size as a function of heating temperature conditions.

Heating temperature conditions (°C) (10 h/stage)	Constant temperature		Consecutive temperature plateaus		
	1000	1200	1000 → 1200	1200 → 1400	1200 → 1400 → 1600
Crystallite size (nm)	74	105	105	109	231

Brought to you by | Karlsruher Institut für Technologie KIT-Bibliothek
Authenticated
Download Date | 6/6/18 7:47 PM

Table 3: Specific surface area (m^2/g) of thorium oxide versus calcination temperature.

Temperature (°C)	Specific area (m^2/g)
850	6.8 ± 0.7
1000	2.6 ± 0.2
1100	2.1 ± 0.2
1200	1.9 ± 0.2
1300	1.6 ± 0.1
1400	1.3 ± 0.1
1500	1.0 ± 0.1

where C ($mg \cdot L^{-1}$) is the measured mass concentration, V (L) the volume and m (mg) the initial ThO_2 mass.

The dissolved mass percentage is then plotted versus the dissolution time. Figure 2 shows a linear evolution of $\%ThO_2$diss versus time until 60% (10 min in this case). The initial dissolution rate corresponds to the slope of this regression line. For times higher that 10 min, a stop in linear evolution is observed and a decrease of the slope of $\%ThO_2$diss versus time is observed. The dissolution rate is defined as the derivative of $\%ThO_2$diss with respect to time. Thus, for contact times lower than 10 min, one can conclude that the dissolution rate is constant. For contact times higher than 10 min, the decrease of the dissolution rate can be explained by the decrease in the surface dissolution active sites. Indeed, the concentration of these surface sites decreases as $\%ThO_2$diss increases (e. g. decreasing of the oxide amount).

In order to easily compare the different dissolution parameters, we have chosen to consider only the linear part of the dissolution curve (as shown on Figure 2) in the present study. Consequently, the dissolution rates are initial dissolution rates, written $V_{diss}(0)$ and expressed in min^{-1}. In the whole text, C_i and $[i]$ will, respectively, represent the total concentration of component i (all the species where i is involved) and the i free species concentration.

3.2.2 Effects of dissolution parameters

Using this methodology, the influences of the specific surface area of solid, the composition of the dissolution medium, and the temperature were studied.

3.2.2.1 Specific surface

As shown in Table 3, specific surface area depends on heating temperature. By varying the synthesis temperature, it was possible to get ThO_2 powder with different specific surface areas. Increasing the firing temperature also impacts on crystallite size, however, this modification can be neglected in the chosen temperature range [20]. The initial dissolution rate was determined for four different specific surface areas and the results are shown on Figure 3. The calcination temperature for this study was chosen ranging between 1100 and 1500°C.

It clearly appears that the initial dissolution rate is proportional to the specific surface area. The initial dissolution rate can thus be written as follows:

$$V_{diss}(0) = K_S.S \quad (2)$$

where K_S ($g/m^2/min$) is the slope of the obtained curve and S (m^2/g) the specific surface area.

It should be noted that the obtained K_s value ($1.4\ g^2/m^2/min$) does not depend on specific surface area,

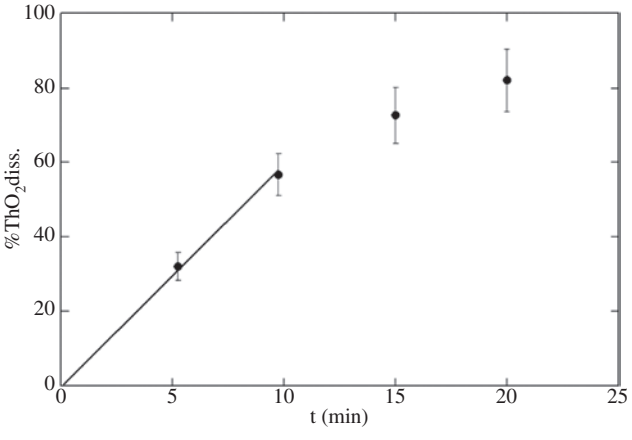

Figure 2: %Dissolved mass of ThO_2 ($\%ThO_2$diss) versus time in 5 mM HF, 5 M HNO_3, 130 mg ThO_2 in 20 mL, 70°C, and specific surface area of 0.9 m^2/g.

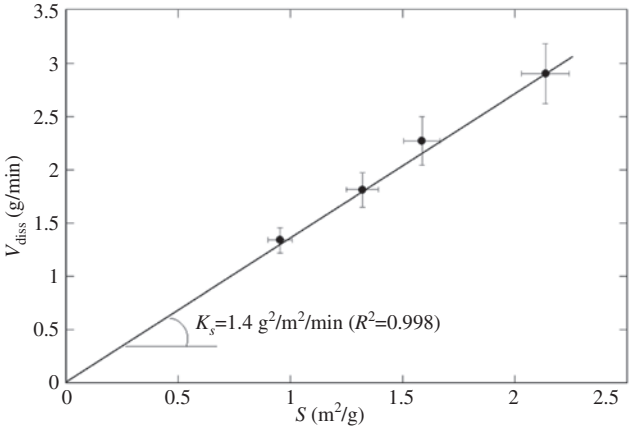

Figure 3: Initial dissolution rate against specific surface area in m^2/g, dissolution medium: HNO_3 5 M HF 5 mM, 50°C.

Brought to you by | Karlsruher Institut für Technologie KIT-Bibliothek
Authenticated
Download Date | 6/6/18 7:47 PM

but it depends on all other parameters and is characteristic of the physico-chemical conditions used here (5 M HNO_3, 5 mM HF, 50°C).

3.3 Dissolution medium

The corrosive effect of the dissolution solution is mainly due to HF. Therefore, H_2SO_4 and $H_2C_2O_4$ were tested as alternative ligand sources. Oxalic and sulfuric acids form stable complexes with Th(IV) [21]. Moreover, sulfuric acid is a strong acid. Considering these two properties, H_2SO_4 was tested alone for dissolution measurements. Thus, the following media were successively considered: $HNO_3/H_2C_2O_4$ and H_2SO_4. Unfortunately, neither for $HNO_3/H_2C_2O_4$ nor H_2SO_4 a meaningful dissolved mass percentage (%ThO_2diss) was obtained after 6 h of stirring at room temperature. Consequently, the study then focused on HNO_3/HF mixtures only. Indeed, it seems that the synergetic effect between HNO_3 and HF is a main interest for the dissolution process.

3.3.1 Influence of HNO_3

Figure 4 presents the dissolved mass percentage as a function of time for several media compositions at 70°C. %ThO_2diss increases with the concentration of nitric acid, showing that HNO_3 plays a major role in the thorium oxide dissolution process. Indeed, a total dissolution of the solid is obtained within 10 min with a mixture of 10 M HNO_3/3 mM HF. Moreover, Figure 4 also shows that the higher the nitric acid concentration, the higher the initial dissolution rate (calculated as already mentioned).

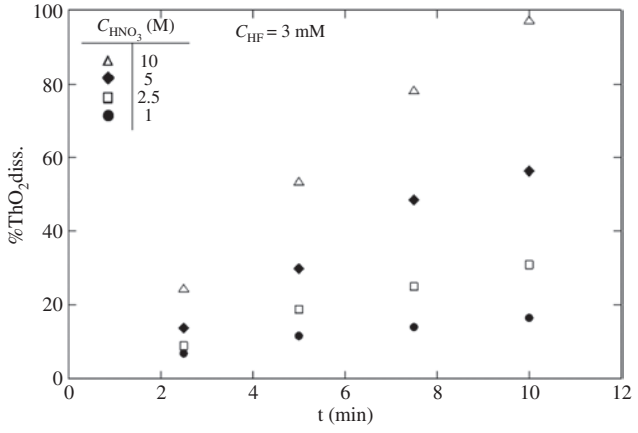

Figure 4: Percentage of dissolved mass versus time at C_{HF} = 3 mM HF at four different nitric acid concentrations, 70°C, 1 m^2/g.

3.3.2 Influence of HF

Figure 5 presents the initial dissolution rate ($V_{diss}(0)$) as a function of hydrofluoric acid concentration measured for nitric acid concentration varying from 1 M to 10 M. As shown in Figure 5, we have delimited three domains (vertical dashed lines). Two domains correspond to $C_{HF} < 15$ mM and a third one to $C_{HF} > 15$ mM. For C_{HF} lower than 15 mM, an increase in the dissolution rate ($V_{diss}(0)$) is observed with increasing HF concentration. Moreover, as it was already evidenced from Figure 4, $V_{diss}(0)$ also depends on HNO_3 concentration. In a first step, for C_{HF} smaller than 3 mM, $V_{diss}(0)$ strongly increases while, in a second step, for C_{HF} ranging from 3 to 15 mM, the slope decreases (e. g. slow increase of the dissolution rate). For HF concentration higher than 15 mM, $V_{diss}(0)$ decreases which a shape depending on nitric acid concentration. The presence of a maximum for $V_{diss}(0)$ whatever HNO_3 concentration proves that an optimal HF concentration exists for the dissolution of thorium oxide. Furthermore, C_{HF} corresponding to the maximum is close to 15 mM for all nitric acid concentrations.

For the highest C_{HF} concentrations, the decrease of $V_{diss}(0)$ is correlated with the formation of a "white precipitate" observed in the solution. In this case, we also obtain a total transformation of thorium oxide to a solid compound which presents a new aspect (color, morphology differences) than thorium oxide. Obviously, the "white precipitate" is formed at the interface solid/solution (corresponding to the maximum of dissolved Th(IV) concentration). It is the reason why we observe a decrease of the dissolution rate and HF, in this concentration range, could appear as a dissolution inhibitor with passivation

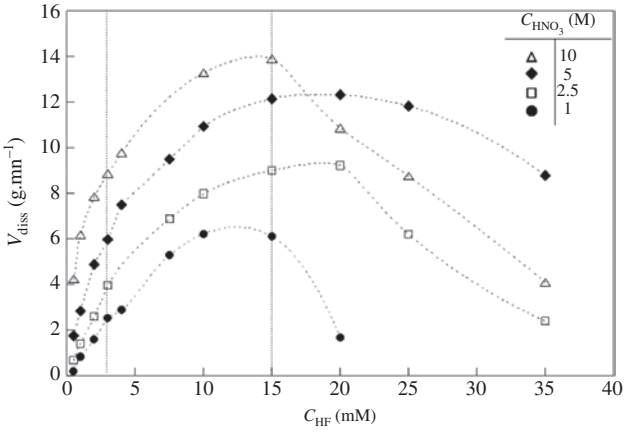

Figure 5: Variation of initial dissolution rates along with HF concentration for several nitric acid concentrations; specific area of 1 m^2/g, 75°C.

Brought to you by | Karlsruher Institut für Technologie KIT-Bibliothek
Authenticated
Download Date | 6/6/18 7:47 PM

of the oxide surface and decrease of the active dissolution sites concentration as it was previously described in the literature in the case of thorium-based compounds such as phosphates [22]. Nevertheless, and because a total dissolution is observed, we suggest that the precipitation occurs at the interface solid/solution after the thorium desorption. That is the only way which allows freeing of active sites of thorium oxide to continue the dissolution. The observation of the precipitate was previously done by Akabori and Shiratori [17] and they only assumed that the precipitate was ThF_4. In this study, in order to identify the nature of the neo-formed phase, XPS experiments were carried out.

A sample corresponding to $C_{HF} = 35$ mM and $C_{HNO_3} = 5$ M was prepared. The "white precipitate" obtained was filtered, and dried at room temperature before being analyzed using XPS [23, 24]. The spectrum of this sample is reported on Figure 6a.

First, we can notice the presence of fluoride in the sample (peak at 685 eV as well as an Auger peak). A small signal corresponding to nitrogen (arising from the nitrate ions) has been found in this sample (peak at 400 eV) but the weakness of this peak suggests that it is not significant.

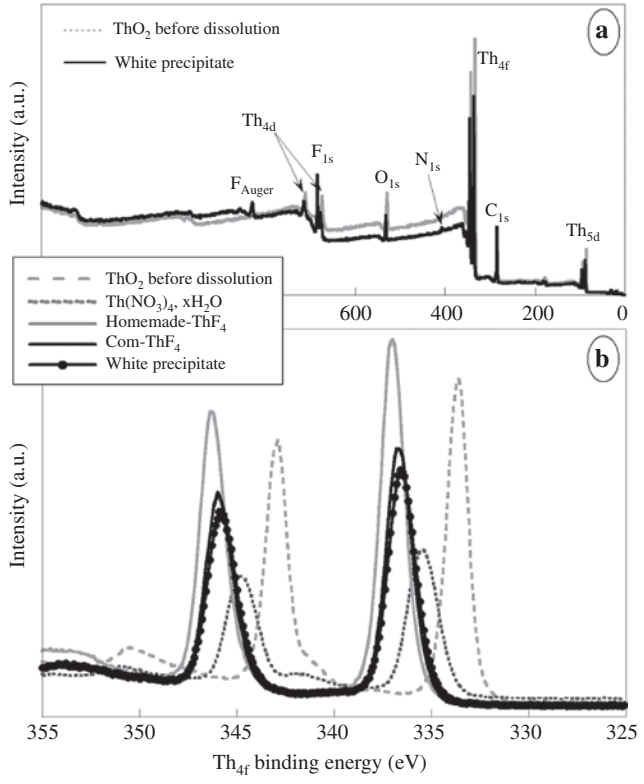

Figure 6: (a) XPS spectra of ThO_2 before precipitation and of the "white precipitate". (b) Comparison of Th_{4f} XPS spectra (reference compounds and precipitate obtained for high HF concentrations).

Carbon and oxygen come from the carbon tape used to fix the sample for the analysis. In order to identify more precisely the nature of the compound, we have recorded with a higher resolution the XPS signal in the region of the Th_{4f} and we have compared the results with in-house reference compounds: thorium nitrate ($Th(NO_3)_3$,xH_2O); thorium oxide before the dissolution process (ThO_2), commercial thorium fluoride (com-ThF_4) provided by SOLVAY and ThF_4 prepared by precipitation of thorium nitrate with HF (homemade-ThF_4). This last sample was prepared in order to have a reference prepared using our chemical conditions. Thus, we have considered an initial thorium solution (in 5 M HNO_3) and we have slowly added concentrated hydrofluoric acid. The obtained precipitate was filtered, and dried at room temperature before analysis.

Figure 6b presents a comparison between Th_{4f} binding energy of the "white precipitate" and those of the reference samples. It is clear that the thorium environment in the "white precipitate" is exactly the same as com-ThF_4 and is very close to the one of homemade-ThF_4. Indeed, if we compare the $Th_{4f7/2}$ electron binding energy ($4f_{7/2}$ BE), the white precipitate presents a $4f_{7/2}$ BE equals to 336.6 eV, the same as com-ThF_4. If we look at the other reference compounds, the homemade-ThF_4 presents a similar $4f_{7/2}$ BE (337.0 eV) as the "white precipitated" but the $4f_{7/2}$ BE obtained for thorium nitrate (335.4 eV) and thorium oxide (333.6 eV) are very far from 336.6 eV. A slight difference is observed between homemade-ThF_4 and the "white precipitate" which could be attributed to the possible co-precipitation of nitrate ions together with fluorides or to the formation of thorium oxy-fluoride compound [25] during the preparation of the homemade-Th solid. Nevertheless, the most important point is to conclude that the observed passivation of the thorium oxide surface for high HF concentrations is due to the formation of thorium tetrafluoride.

Since the presence of ThF_4 is evidenced for high HF concentration, we can reasonably propose that the observed diminution of $V_{diss}(0)$ increases for hydrofluoric acid concentrations ranging from 3 to 15 mM could also be due to the starting formation of such a precipitate which does not completely cover the ThO_2 surface. The formation of a very thin surface layer could also lead to a slowdown in dissolution rate without a complete stop of the dissolution reaction.

The ThF_4 solubility results have been compiled by OECD [26] (Figure 7). The solubility of ThF_4 is plotted as a function of free fluoride ions concentration ($[F^-]$) at 50°C in 4.6 M HNO_3. As only the total HF concentration is fixed in our study, the free fluoride ions concentration has to be estimated to compare with our results.

Brought to you by | Karlsruher Institut für Technologie KIT-Bibliothek
Authenticated
Download Date | 6/6/18 7:47 PM

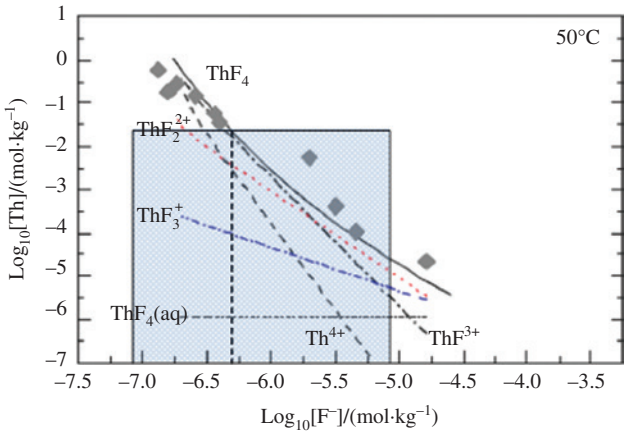

Figure 7: Thorium speciation and ThF_4 solubility as a function of fluoride concentration, 50°C, 4.6 M HNO_3, figure taken from OECD vol 11 [21].

Thus, $[H^+]$ concentrations and a HF dissociation constant (pK_a (HF) = 3.2 at 25°C) are required. The total concentration of $[H^+]$ is given by the sum of protons released by HNO_3 and HF acids. Considering α_1 and α_2 as the dissociation coefficients of HF and HNO_3, respectively, one can write:

$$[H^+] = \alpha_1 . C_{HF} + \alpha_2 \cdot C_{HNO_3} \quad (3)$$

The nitric acid concentrations range from 1 to 10 M while those of HF never exceed 50 mM, then we can neglect the first term in equation (3). Thus, the dissociation equation for HF can be written as follows:

$$\underset{C_{HF}(1-\alpha_1)}{HF} \rightarrow \underset{\alpha_1 C_{HNO_3}}{H^+} + \underset{\alpha_1 C_{HF}}{F^-} \quad (4)$$

Thus, the dissociation constant of HF becomes:

$$K_a(HF) = \frac{\alpha_1 C_{HF} \cdot \alpha_2 C_{HNO_3}}{C_{HF}(1-\alpha_1)} \quad (5)$$

And the free fluoride ion concentration is given by:

$$[F^-] = \alpha_1 C_{HF} = \frac{K_a(HF) \cdot C_{HF}}{K_a(HF) + \alpha_2 C_{HNO_3}} \quad (6)$$

The term $\alpha_2 \cdot C_{HNO_3}$ was calculated from the dissociation coefficients of nitric acid reported by Davis et al. [27].

Using relation (6), we have defined on Figure 7 a light gray rectangle which corresponds to our experimental conditions. The upper horizontal line represents the concentration of thorium obtained when total dissolution occurs (24.6 mM). The two vertical lines represent the limits of the fluoride ions concentrations used in this study (from 0.5 to 50 mM of total HF).

The dashed vertical line was drawn for a total HF concentration of 3 mM. We can observe that this line intercepts the solubility curve of thorium tetrafluoride for a thorium concentration equals to 24.6 mM. It means that up to a HF concentration of 3 mM, a total thorium oxide dissolution can be achieved. For higher HF concentration, the formation of precipitated ThF_4 leads to an incomplete dissolution. This observation is in good agreement with the experimental results obtained concerning the variation of the dissolution rate as a function of HF total concentration and the formation of ThF_4 for high concentrations of HF.

3.4 Dissolution methods

The most commonly used dissolution way consists in solubilizing metallic ions in an aqueous medium while stirring and heating. The effects of these two parameters on dissolution have thus been studied. To ensure the accuracy of the results, both nitric acid and hydrofluoric acid concentrations have been fixed for each experiments, except for those where concentration variation were specifically studied. Concentration values of 5 M and 5 mM have been chosen for HNO_3 and HF, respectively, except in cases where very low dissolution rates were required. In this case, 1 M HNO_3 and 3 mM HF were used.

3.4.1 Stirring effect

While the literature claims that the stirring speed does not impact thorium oxide dissolution [16, 28], we have observed a slight decrease of $\%ThO_2$diss without stirring

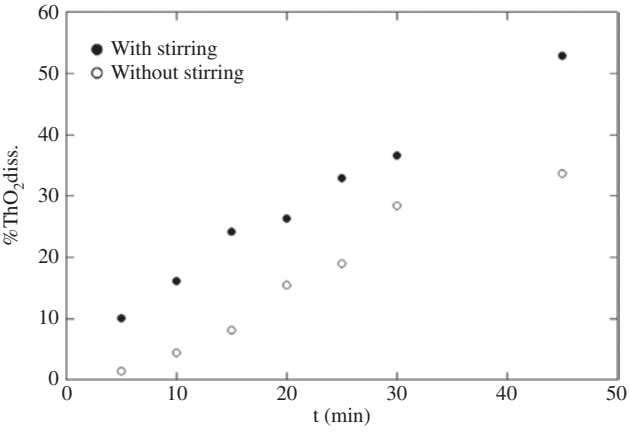

Figure 8: %Dissolved mass versus time with and without stirring, 130 mg ThO_2 in 20 mL, 1 M HNO_3, 3 mM HF, specific surface area 1.5 m^2/g.

Brought to you by | Karlsruher Institut für Technologie KIT-Bibliothek
Authenticated
Download Date | 6/6/18 7:47 PM

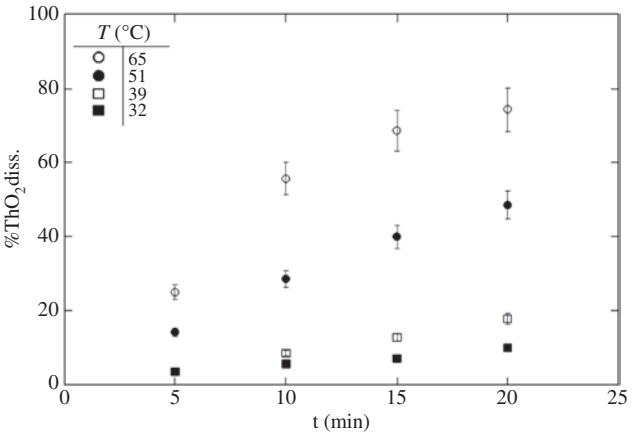

Figure 9: %Dissolved mass versus time obtained at several temperatures, 10 M HNO_3, 5 mM HF, specific surface area of 1.5 m^2/g, 130 mg ThO_2 in 20 mL.

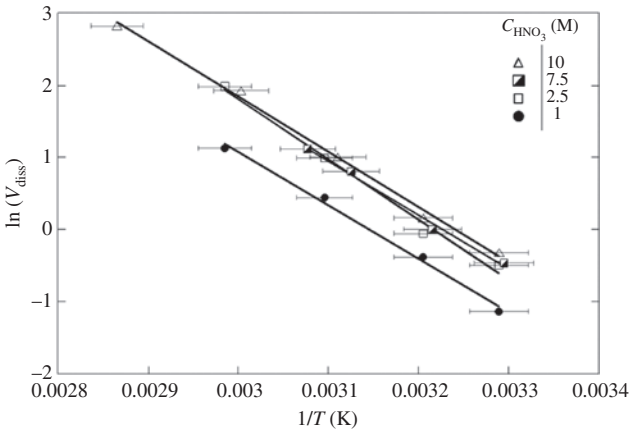

Figure 10: Arrhenius plot for different HNO_3 concentrations, 5 mM HF and temperatures ranging from 30 to 70°C.

(Figure 8) due to a time shift in the dissolution process. Nevertheless, the slopes of the curves reported on Figure 8 seem to be the same which indicates that the dissolution rates are similar with and without stirring. Even if stirring is not a key parameter for the total dissolution achievement, and for more reliable conditions, further experiments were achieved with stirring.

3.4.2 Temperature effect

Figure 9 presents the variation of ThO_2 dissolution as a function of time at four different temperatures (from 30 to 70°C), clearly showing dissolution proceeds faster at higher temperature. The higher is the temperature, the higher is the slope.

Thorium dioxide dissolution follows the Arrhenius law [9]: the logarithm of the initial dissolution rate is linked to the temperature reciprocal with the following formula:

$$\ln(V_{\text{diss}}(0)) = \text{Cst} - \frac{E_a}{RT} \quad (7)$$

where E_a is the activation energy in $J \cdot mol^{-1}$, T is the temperature in K, Cst a constant and R the ideal gas constant equal to 8.314 $J \cdot mol^{-1} \cdot K^{-1}$.

Measurements of the initial dissolution rates were made for several nitric acid and hydrofluoric acid concentrations at four different temperatures. Initial dissolution rate logarithms were plotted versus temperature reciprocal for each experiment. Straight lines were always observed. Figure 10 shows results at four different nitric acid concentrations and for a total HF concentration of 5 mM.

The curves analysis leads to the determination of the activation energies, according to the relation (7). The measured activation energy values for a known total HF concentration and for HNO_3 concentration ranging from 1 to 10 are gathered in Table 4. No clear dependence of E_a versus C_{HNO_3} has been observed leading to a mean activation energy value of 63 $kJ \cdot mol^{-1}$.

In a second series of experiments, the total HNO_3 concentration was kept constant while the HF concentration was varied. All the measured activation energy values are reported on Figure 11, plotted as a function of the total HF concentration. Until 10 mM HF, a first plateau is observed (E_a close to 60 $kJ \cdot mol^{-1}$) and for concentrations higher than 20 mM, a second plateau is obtained (E_a close to 80 $kJ \cdot mol^{-1}$).

Values obtained in the present work are in the same range as previous studies [1, 16, 17, 28] in which values are close to 70 $kJ \cdot mol^{-1}$. Unfortunately, no data relative to the variation of activation energy along with nitric acid experiments are available in the literature. Akabori and Shiratori [17] observed that activation energy increases with increasing hydrofluoric acid concentration. Their results ranged from 35 $kJ \cdot mol^{-1}$ to 105 $kJ \cdot mol^{-1}$ for HF concentrations from 1 mM to 50 mM but they studied a higher temperature range (until 150°C). Contrary to them, in our study (Figure 11), the activation energy has

Table 4: Activation energy values depending on nitric acid concentration at C_{HF} 5 mM; studies on a 1.5 m^2/g specific area thorium oxide, 130 mg in 20 mL.

C_{HNO_3} (M)	1	2.5	5	7.5	10
E_a (kJ/mol)	59 ± 5	61 ± 5	63 ± 5	64 ± 5	65 ± 5

Brought to you by | Karlsruher Institut für Technologie KIT-Bibliothek
Authenticated
Download Date | 6/6/18 7:47 PM

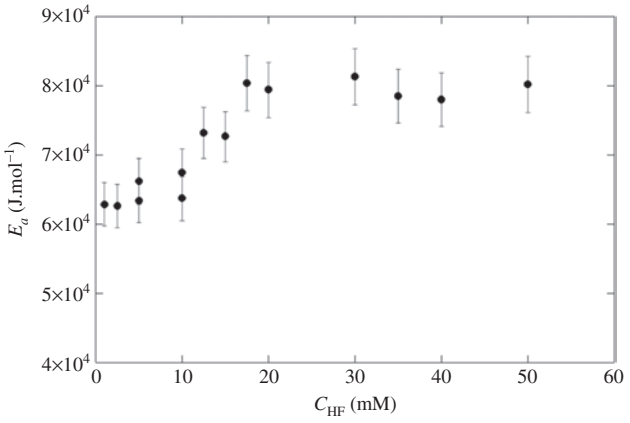

Figure 11: Activation energy versus hydrofluoric acid concentration, C_{HNO_3} 5 M; studies on a 1.5 m²/g specific area thorium oxide, 130 mg in 20 mL.

remained at an almost constant value of 63 kJ·mol^{-1} for hydrofluoric acid concentration from 0.5 mM to 10 mM. We then observe a slight increase to reach an activation energy value of around 80 kJ·mol^{-1} at HF concentration equal to or higher than 20 mM. This difference can be explained by the formation of ThF_4 as demonstrated already, which impacts the dissolution rate, resulting in variation of the activation energy. We can thus expect that in Akabori and Shiratori experimental conditions, ThF_4 also formed, though they found a sharper increase in activation energy (35–105 kJ·mol^{-1}) than in our study (63–80 kJ·mol^{-1}). The difference between Akabori's higher value (105 kJ·mol^{-1}) and ours (80 kJ·mol^{-1}) could probably arise from the value of the highest temperature considered in both studies (150°C for Akabori and 70°C in this study).

As a conclusion, the activation energy value characteristic of the dissolution mechanisms in optimal conditions, which means without ThF_4 formation, is equal to 63 kJ/mol.

The activation energy calculated from the Arrhenius plot seems characteristic of a mechanism limited by a surface reaction. Indeed, the expected value for pure diffusion-controlled phenomena is about 20 kJ·mol^{-1} [29]. The direct breaking of covalent bound requires energy ranged between 160 and 400 kJ·mol^{-1}. Activation energy values for processes controlled by adsorption are higher than 80 kJ·mol^{-1} [30]. However, if a catalytic reaction is involved in the dissolution mechanism, a decrease of the activation energy is observed. In our case, the measured energy is likely characteristic of a mechanism controlled by an adsorption reaction associated with a catalytic effect. The experiments have demonstrated the strong influence of very low concentrations of HF on the kinetic dissolution and we observe an activation energy which could be consistent with a catalytic effect. For further studies, the role of HF has to be more precisely analyzed to confirm these assumptions.

4 Conclusion

A multi-parametric study performed on ThO_2 powder solubilization has shown that the rate of dissolution process is directly proportional to the specific surface area of the substrate. It was shown that only stirring and heating are pertinent parameters for thorium oxide dissolution. The chemical conditions were also varied in order to investigate the influence of acids and ligands towards ThO_2 dissolution. Fluoride ions, associated with another acid (in our case nitric acid), have been found to lead to the best dissolution rate compared to other complexing agents towards thorium such as oxalate or sulfate ions. The existence of an optimum HF concentration for ThO_2 dissolution has also been demonstrated. Indeed, when no HF is added to the system, no complete dissolution can be achieved as well as when too much hydrofluoric acid is used. The optimum HF concentration is around 3 mM. This concentration is a good compromise between the dissolution rate and ThF_4 formation prevention. In order to understand why a high HF concentration leads to an incomplete dissolution, XPS experiments were performed. It was shown that in such conditions thorium tetrafluoride is formed at the interface. The influence of nitric acid was also investigated. High HNO_3 concentration yields faster dissolution but this acid could not lead to a complete thorium oxide dissolution when no HF is added to the system, which evidences the synergetic effect of HF and HNO_3. The role of HF requires more studies and the reaction mechanism has to be determined. The value of activation energy tends to suggest a mechanism controlled by an adsorption reaction combined with a catalytic reaction.

In order to propose optimal conditions to improve THOREX process, the knowledge of the kinetic mechanism is required and particularly the effect of the mass/volume ratio which is a key parameter not yet studied.

Acknowledgments: The authors would like to thank AREVA and the CNRS for financial support.

Brought to you by | Karlsruher Institut für Technologie KIT-Bibliothek
Authenticated
Download Date | 6/6/18 7:47 PM

References

1. Farrel, M. S., Isaacs, S. R.: Dissolution of Urania – Thoria fuel particles in nitric acid solutions. Australian Atomic Energy Commission Research Establishment Lucas Heights. AAEC/E143 (1965), Sydney.
2. Lung, M.: A present review of the thorium nuclear fuel cycles. nuclear science and technology. s.l.: Nuclear Science and Technology, European commission, EUR 17771 EN (1997), Luxembourg.
3. Lung, M., Gremm, O.: Perspectives of the thorium fuel cycle. Nucl. Eng. Des. **180**, 133 (1998).
4. Gresky, A. T.: Solvent extraction separation of U233 and thorium from fission products by mean of TBP. Proceedings of the International Conference on the Peaceful Uses of Atomic Energy **9**, 505 (1955).
5. Lyczko, K., Lyczko, M., Walo, M., Lipkowski, J.: Conversion of Th(IV) oxide into Th(IV) trifluoromethanesulfonate: crystal structure of Th(IV) trifluoromethanesulfonate dihydrate. Inorg. Chem. Com. **24**, 234 (2012).
6. Mirashi, N. N., Chaudhury, S., Aggarwal, S. K.: Dissolution of sintered thorium dioxide in phosphoric acid using autoclave and microwave methods with detection by gamma spectroscopy. Microchem. J. **94**, 24 (2010).
7. Malav, R. K., Save, N. D., Prakash, A., Afzal, Md., Panakkal, J. P.: Use of indigenous microwave system for dissolution and treatment of waste nuclear materials. J. Radioanal. Nucl. Chem. **295**, 425 (2013).
8. Sato, N., Kirishima, A.: Sulfurization behavior of thorium dioxide with carbon disulfide. J. Nucl. Mater. **414**, 324 (2011).
9. Heisbourg, G., Hubert, S., Dacheux, N., Ritt, J.: The kinetics of dissolution of $Th_{1-x}U_xO_2$ solid solutions in nitric media. J. Nucl. Mater. **321**, 141 (2003).
10. Hingant, N., Clavier, N., Dacheux, N., Hubert, S., Barre, N., Podor, R.: Preparation of morphology controlled $Th_{1-x}U_xO_2$ sintered pellets from low-temperature precursors. Powder Technol. **208**, 454 (2011).
11. Hubert, S., Barthelet, K., Fourest, B., Lagarde, G., Dacheux, N., Baglan, N.: Influence of the precursor and the calcination temperature on the dissolution of thorium dioxide. J. Nucl. Mater. **297**, 206 (2001).
12. Claparede, L., Tocino, F., Szenknect, S., Mesbah, A., Clavier, N., Moisy, P., Dacheux, N.: Dissolution of $Th_{1-x}U_xO_2$: effects of chemical composition and microstructure. J. Nucl. Mater. **457**, 304 (2015).
13. Martinez, J., Clavier, N., Ducasse, T., Mesbah, A., Audubert, F., Corso, B., Vigier, N., Dacheux, N.: From uranium(IV) oxalate to sintered UO_2 : consequences of the powders' thermal history on the microstructure. J. Europ. Ceram. Soc. **35**, 4535 (2015).
14. Brunauer, S., Emmett, P. H., Teller, E.: Adsorption of gases in multimolecular layers. J. Am. Chem. Soc. **60**(2), 309 (1938).
15. Pickett, J. B., Fowler, J. R., Clanton Mosley, W. Jr: Roasting and dissolution studies on non irradiated thorium dioxide/uranium dioxide pellets. DP-1590: E. I. du Pont de Nemours. & Co., Savannah River Laboratory, SC 29808 (1982), Aiken.
16. Takeuchi, T., Hanson, K. C., Wadsworth, M. E.: Kinetics and mechanism of the dissolution of thorium oxide in hydrofluoric acid and nitric acid mixtures. J. Inorg. Nucl. Chem. **33**, 1089 (1971).
17. Akabori, M., Shiratori, T.: Dissolution of ThO_2-based oxides in nitric acid solutions at elevated temperatures. J. Nucl. Sci. Technol. **31**, 539 (1993).
18. Lomenech, C., Drot, R., Simoni, E.: Speciation of uranium(VI) at the solid/solution interface: sorption modelling on zirconium silicate and zirconium oxide. Radiochim. Acta **91**, 453 (2003).
19. Haleem Khan, M., Ali, A., Niaz Khan, N.: Spectrophotometric determination of thorium with dissodium salt of arsenzao-III in perchloric acid. J. Radioanal. Nucl. Chem. **250**(23), 353 (2001).
20. Claparède, L., Clavier, N., Dacheux, N., Mesbah, A., Martinez, J., Szenknect, S., Moisy, P.: Multiparametric dissolution of thorium-cerium dioxide solid solutions. Inorg. Chem. **50**, 11702 (2011).
21. Oktay, E., Yayli, A.: Physical properties of thorium oxalate powders and their influence on the thermal decomposition. J. Nucl. Mater. **288**, 76 (2001).
22. Clavier, N., du Fou de Kerdaniel, E., Dacheux, N., Le Coustumer, P., Drot, R., Ravaux, J., Simoni, E.: Behavior of thorium-uranium (IV) phosphate-diphosphate sintered samples during leaching tests. II- Saturation processes. J. Nucl. Mater. **349**, 304 (2006).
23. Cakir, P., Eloirdi, R., Huber, F., Konings, R. J. M., Gouder, T.: An XPS and UPS study on the electronic structure of ThO_x ($x \leq 2$) thin films. J. Phys. Chem. C. **118**, 24497 (2014).
24. Teterin, A. Y., Ryzhkov, M. V., Teterin, Y. A., Vukcevic, L., Terekhov, V. A., Maslakov, K. I., Ivanov, K. E.: Nature of chemical bonding in ThF_4. Radiochemistry **51**(6), 551 (2009).
25. D'eye, R.: The thorium dioxide-thorium tetrafluoride system. J. Chem. Soc. 196 (1958).
26. Rand, M., Fuger, J., Grenthe, I., Neck, V., Dhanpat, R.: Chemical thermodynamics of thorium. Chemical thermodynamics Vol. 11. OECD, 2007, Issy-Les-Moulineaux, France.
27. Davis, W., De Bruin, H. J.: New activity coefficients for 0–100 percent aqueous nitric acid. J. Inorg. Nucl. Chem. **26**, 1069 (1964).
28. Shying, M. E., Florence, T. M., Carswell, D. J.: Oxide dissolution mechanisms I. J. Inorg. Chem. **32**, 3493 (1970).
29. Glatz, J. P., Bokelund, H., Zierfuβ, S.: Analysis of the off-gas from dissolution of nuclear oxide- and carbide fuels in nitric acid. Radiochimica. Acta **51**, 17 (1990).
30. Tocino, F., Szenknect, S., Mesbah, A., Clavier, N., Dacheux, N.: Dissolution of uranium mixed oxides: the role of oxygen vacancies vs the redox reactions. Prog. Nucl. Energy **72**, 101 (2014).

Brought to you by | Karlsruher Institut für Technologie KIT-Bibliothek
Authenticated
Download Date | 6/6/18 7:47 PM